Performance Test of Multi Micro-Channel Evaporators for Cooling a High Heat Flux Electronic Devices

[1]MOHAMED KARIM, [2]A.M.K EL-GHONEMY, [3]ELDESOUKI I. EID

[1]Egyptian Russian University, EGYPT
[2]High Institute of Engineering and Technology, EGYPT
[3]Suez canal university, EGYPT

Abstract: Multi rectangular micro-channel evaporators is one of the promising technologies for cooling the new generation of electronic chips with high heat flux to maintain its safe temperature at low energy consumption.Where, it improves the heat transfer coefficient athigher mass velocities.The present study is directed to measure and evaluate the performance of a conventional microchanel evaporator (Case-1), orifice at inlet to microchanel evaporator(Case-2) and tree at inlet to microchanel evaporator (Case3). Where, the performance indicators are presented to compare between the proposedthree cases in terms of heat transfer coefficient, pressure drop and wall temperature. The results showed that,The highest record of heat transfer coefficient (h=109 KW.m-2.K-1) is obtained at mass flux of (G=900Kg.m-2.S-1) from case-3.

Keywords: electronic cooling, microchanels evaporators performance, experimental study

Nomenclature:

A	area (m²)
Bo	Bond number
Bl	boiling number
Dh	hydraulic diameter (mm)
G	mass flux (kg m−² s−¹)
g	gravitational acceleration
H	height (m)
L	length (m)
h	heat transfer coefficient (kW m−² K−1)
i	enthalpy (kJ kg−¹)
$\dot{m}$	mass flow rate (kg s−¹)
N	number of channels
Pr	Prandl number
Re	Reynolds number
T	temperature (°C)
q″	heat flux (kW m−2)
Q	heat transfer rate (kW)
x	vapor quality
W	width

Greek letters

η	fin efficiency
ρ	density (kg m−³)
μ	viscosity (kg m−¹ s−¹)
σ	surface tension (N m−¹)
∅	two-phase frictional multiplier
ε	surface roughness parameter

Subscripts

ave	average
b	base
c	copper
CB	convective boiling
ch	channel
fin	fin
in	inlet
l	liquid
lo	liquid only
sat	saturated
TP	two-phase
w	wall
v	vapor
vo	vapor only
η	fin efficiency
ρ	density (kg m−³)
μ	viscosity (kg m−¹ s−¹)
σ	surface tension (N m−¹)

Introduction

Electronic devices are widely used in different applications such as computers, communications, biomedical, automotive, military and aerospace. The performance and reliability of electronic devices are known to increase when operating temperatures are kept below 50°C.

According to the International Technology Roadmap for Semiconductors (ITRS), the future generationof high-performance electronic chips will leads to a high increase in power density. Consequently, leads to a high heat flux density of high-speed electronic devices. Electronic products are classified into five major categories based on the characteristics and demands of their application domains: 1: low cost, 2: handheld (portable), 3: cost performance, 4: high performance, 5: harsh environment.

The major causes of electronic failures are presented in fig.(1). As highlighted in this figure, the thermal one is the major cause of electronic failure.

Different electronic chip cooling methods Such as Free convection, heat spreaders, interface materials, air cooled heat sinks, liquid cooled cold plates, direct immersion cooling, vapor compression, solid state refrigeration are summarised in table(1).

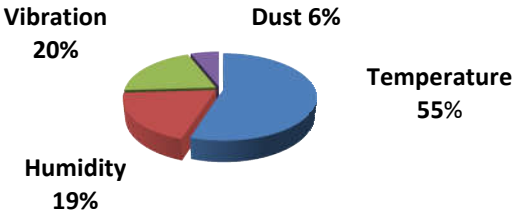

Fig.1: Major causes of electronic failure[1].

Conventional cooling techniques cannot cope with this continuous increase in cooling needs of such compact and high heat generating electronic devices. Therefore, new cooling systems are required such as microchannels evaporators in a cooling systems.

Various small and mini heat exchangers are defined in terms of hydraulic diameter Dh, as:

-Micro heat exchanger: Dh = 1–100 µm.
-Meso heat exchanger: Dh = 100 µm to 1 mm.
-Compact heat exchanger: Dh = 1–6 mm.
- Conventional heat exchanger: Dh> 6 mm

Kandlikar[3-8]defined the following ranges of hydraulic diameters Dh :-

-Dh>3 mm.
-Minichannels: Dh = 200 µm to 3 mm.
-Microchannels: Dh = 10–200 µm

Micro-channel heat sinks are devices that provide liquid flow through parallel channels having a hydraulic diameter of around 5–500µm. High-

heat flux thermal management schemesincludesultra high-heat fluxes in the range of 1,000–100,000W.cm^{-2}[3]. A micro-channel heat sink can be classified as single-phase or two-phase according to the state of the coolant inside it.

The present subject has been studied by many authors[1-22].However most of the published articles are related to using single phase fluid as a cooling medium in microchannel evaporators. From reviewing the related literatures [1-22], the following points have been focused by researchers:

- Flow boiling heat transfer, flow regime maps, boiling curves in conventional and micro scale, and two phase flow.
- Flow in microchannels and two-phase flow boiling.
- Pressure drop reduction in micro evaporators.
- Refrigerant mal-distribution in microchannel heat exchanger.
- Potential options to improve refrigerant distribution.
- Separation of two-phase flow after expansion.
- Reverse vapor flow and boiling fluctuations.
- Design and Modeling of micro evaporators.

Nowadays, thermal management of electronic cooling is becoming more important. Where, the power dissipation from high performance microprocessor chips will reach about 360 W by 2020 [1].

Table 1: Chip cooling methods

Chip category	Chip cooling
Low cost	Free Convection
Hand held	Free Convection + heat spreaders
Cost performance	Free Convection + heat sinks
High performance	Free Convection + heat sinks +heat pipes+ liquid
Harsh environment	All together

Finally, From the Previous studies[1-22],the following questions are concluded to be considered in the present researches:

1. How to reduce the pressure drop in the micro-evaporator?
2. How check an equal distribution in the micro-evaporator?
3. How to reduce the bubbles to avoid blockage of the entrance or inside the micro-evaporator?
4. How to reduce the flow of steam and boiling reverse fluctuations in the micro-evaporator?

Based on the above mentioned questions, the present paper is directed to study experimentally the performance of three different geometries of micro-channelevaporators:-

The first geometry (Case-1) is using a conventional micro-channel evaporators with divergent shape in the flow direction (fig.3a).While, The second geometry (Case-2) is using an orifice at inlet to each micro-channel path, fig.(3b). Finally, the third geometry (Case-3) is using a tree at inlet to microchannel paths, fig(3c).

The performance of the studied three cases is tested experimentally and evaluated in terms of: Heat transfer coefficient, pressure drop, and wall temperature under different mass

fluxes and different constant heat fluxes.

Experimental setupand measurement techniques

In order to evaluate the performance of the studied three cases of microchannel evaporator, Major components and instrumentation will be presented**.**

Figure (4) shows a diagram of the experimental setup which is a normal refrigeration system. The cooling cycle has been designed to ensure the entry of the expansion valve is almost in liquid phase by using the T - junction which separators the refrigerant gas to be bypassed intothe compressor inlet. Also an oil separator is used to minimize the effect of oil flow with refrigerant into evaporator.

The refrigerant flow rate is measured at the condenser outlet by a Rotameter type flow meter.Refrigerant quality at inlet to the test section is calculated from measuring T and P at inlet to test sections. pressures and temperatures are measured by bourden tube gages(P) and T-type thermocouples (T). Vapor and liquid refrigerant are separated in the T-junction located before the expansion valve. A needle valve is directly connected at the inlet to test samples which is used for changing the mass flux. The microchannel evaporator (test samples) heat sink was sandwiched between the top cover from transparent Pyrex glass material and the built in bottom frame as shown in Figure 3. Each test sample and its built in bottom frame are made from copper material. The top frame is a transparent polycarbonate plastic with a thermal conductivity of 0.19 $W.m^{-1}K^{-1}$ and a maximum service temperature of 120 °C. Thermal insulation are made for both the top and the bottom frames to avoid heat losses. Electrical connections for the heater and the sensors are made in the proper way and sensors probes inserted in the holes drilled in the bottom frame. Figure 4.ashows, the inlet and outlet fluid temperatures were measured by high-precision T-type thermocouples with a hole diameter of 1.0 mm; the resolution of the thermocouple reader was ±0.1°C. All the thermocouples and pressure gauges were calibrated before use. A needle valve fitted directly at inlet to evaporator allows for fine adjustment of the flow rate, which corresponds to a mass fluxes of [400,900 and 1300 $Kg.m^{-2}.S^{-1}$]. 7 holes of 8.0 mm diameter were drilled in the copper block to accommodate the cartridge heaters. The cartridge heater was powered by a 0–220 V AC Variac, and the heating power was measured by a precision digital wattmeter with an accuracy of 0.1%.

All the measured parameters and its location are summarized in table(2)

Table(2-a): detailed dimensions of the test sections

Parameters	**Dimensions**
Number of channels (N)	32
Hydraulic diameter (Dh)	125µm
Channel width (Wch)	165 ± 1 µm
Channel depth (Hch)	100± 1 µm
Aspect ratio (β)	0.70
Channel length (L)	20 mm
Distance from thermocouple to the channel base (δ)	3 ± 0,025 mm

T
Ta

Table-2b: the measured parameters and its location

instrument	location
Pressure	Inlet to and oulett from the test section And comprosser and condenser and heatexangher and expanstion valve
temperatures	Inlet to and oulett from the test section And comprosser and condenser and heatexangher and expanstion valve and wall section test
Rotameter flow	Out let of condenser
Wattmeter	heater

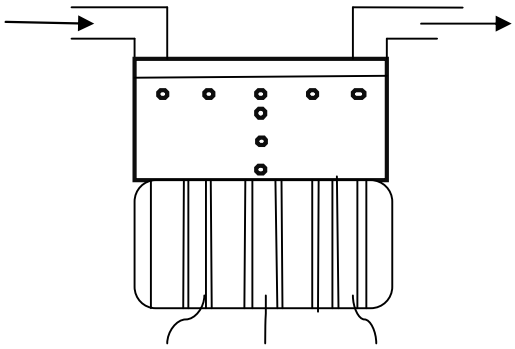

Fig.(2): Thermocouple locations in the test section(plan view)

Three test sections (evaporators) were designed using SOLIDWORKS software (CAD), Then The G-M code was generated and executed by using The CNC laser cutting machine (CAM). Where,the three test sections were made of copper. There are 32 arrays of the parallel microchannel in each evaporator, each having 139 μm width with a constant depth of 200 μm. The inlet and outlet plenums have a constant width of 8 mm and depth of 200 μm manifolds. T-type thermocouples were inserted in the inlet and outlet plenums of the microchannel, at equal distances of 5 mm to measure the temperature distribution within the plenums. [Figure-3] contains schematic drawings of the three test sections. A divergent channel reduces fluid acceleration and achieve a stable boiling process.

Seven immersion heaters with the total power of 1050 W were installed inside the copper block. The heaters were controlled using a PI temperature controller sensed by a K-type thermocouple.

A schematic with dimensions of each case is shown in fig.(3). Also, a photo of each sample is included.

Data reduction

The steady state performance parameters of microchannel evaporators can be calculated as follows [8-10]:

$$Q_{total} = Q_{fluid} + Q_{loss}$$

Q_{total} is the total heat supplied by the electric heater, $Q_{fluid}$is the heat removed by the fluid, and $Q_{loss}$is the

heat loss. The total heat obtained directly as $Q_{total}= V\ I$ where$V$ is the voltage and I is the current in the heater.The net heat transfer rate (Q_{net})supplied to the working fluid in the microchannel heat sink is calculated as follow:

$$Q_{net} = m_r * (h_{out} - h_{in})$$

i-The wall heat flux is obtained:

$$q_W^{"} = \frac{Q_{net}}{A_t}$$

Where,

$Q_{net}$is the net heat transfer rate to the fluid, and

ii-$A_t$is the total heated area of the microchannels which is:

$$A_t = N(w + 2d)\ L$$

Where L is the microchannel length, *w* is The width, *d* is the depth, and N is the number of microchannels.

iii-The local heat transfer coefficient, *h* is:

$$h = \frac{q_W^{"}}{\eta_o\,(T_w - T_{ref})}$$

Where:

T_{ref}: is the local mean fluid temperature (for single-phase) and the liquid saturation temperature (for two-phase region), K.

T*w*: is the local wall temperature, K

η_o: is the overall surface efficiency. Based on the microchannel width and depths, η_o is estimated to be in the range between: 96.7% : 99.9% [1].

iv-Non-dimensional parameters used for flow boiling are: Reynolds number (Re), Bond number(Bo) and boiling number (Bl). Each parameter is calculated as follows:

a- Using the liquid phase mass flux, Reynolds number can be calculated as:

$$\mathrm{Re} = GD/\mu$$

Where:

μ: is the dynamic viscosity of the liquid.

b- Bond number:

$$\mathrm{Bo} = g(\rho_f - \rho_g).\, D^2/\sigma$$

where

ρ_f , ρ_g are the density of the liquid and vapor phases, respectively, and

σ : is the liquid surface tension

c- Boiling number

$$Bl = \frac{q_W^{"}}{G\,(h_{fg})}$$

Where h_{fg} is latent heat,

d-Finally thepressure drop is: P_{in}- P_{out}

e-the vapor quality is:

The evaporator's inlet quality, x_{in}, is estimated from the enthalpy value and the evaporator's inlet temperature or pressure measurements.

$$x = \frac{h}{h_{fg}}$$

the pressure drop of the microchannel is calculated by (including sudden contraction and sudden expansion at the inlet and outlet of the microchannels):

$$\Delta P = P_{in} - P_{out}$$

The mass flux (G) is calculated by:

$$G = \frac{m^o}{N.A_{in}}$$

Where A_{in} is the cross section area of a single microchannel inlet.

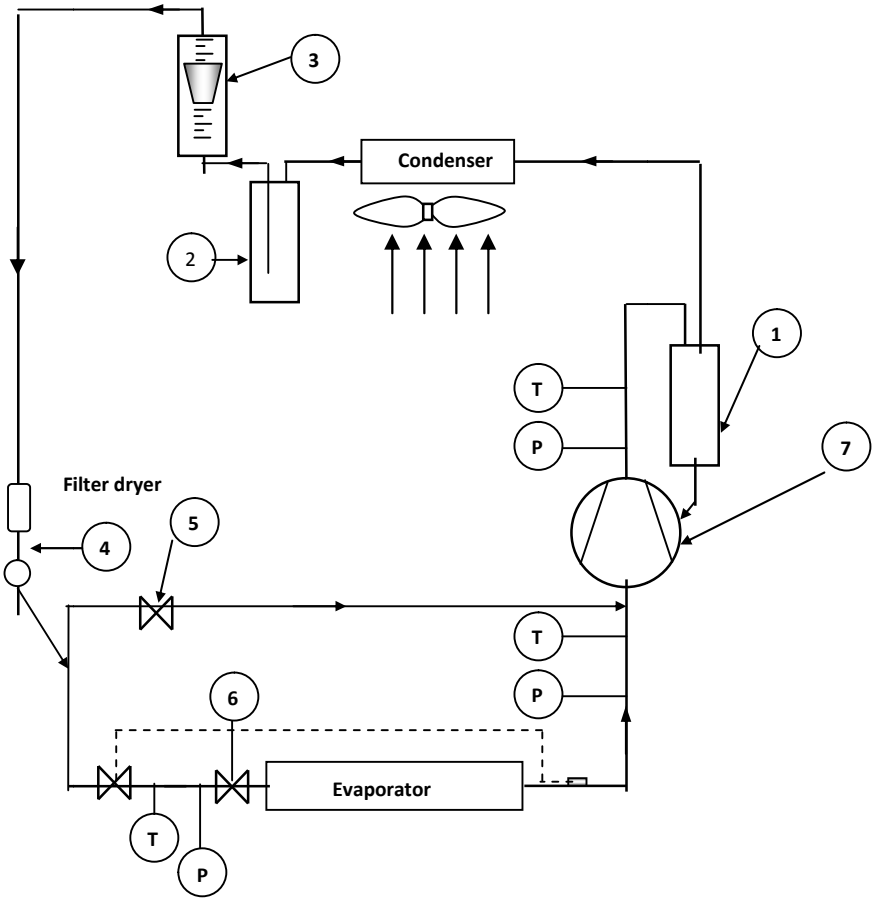

Fig (4-a): Schematic diagram of the experimental setup using R-134a
1. oil separator, 2. Liquid accumulator, 3. flow meter, 4. Sight glass, 5. Gas valve ,6. Nedle Valve, 7. Compressor.

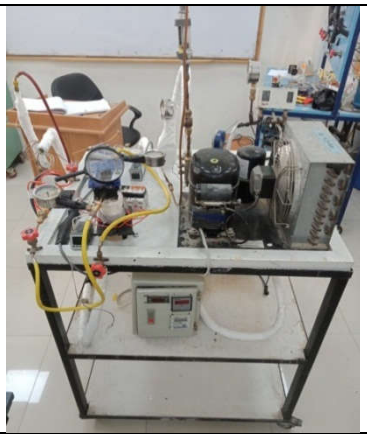

Figure(4b): Photo of the test rig and layout

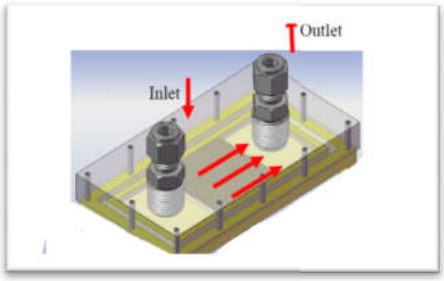

Figure(4c): Inlet and outlet flow directions

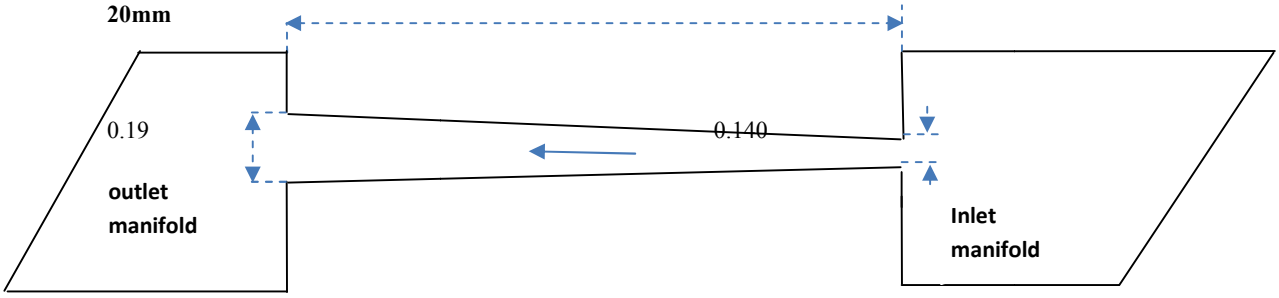

Fig.(3a): geometrical dimensions of Case-1 (one path)

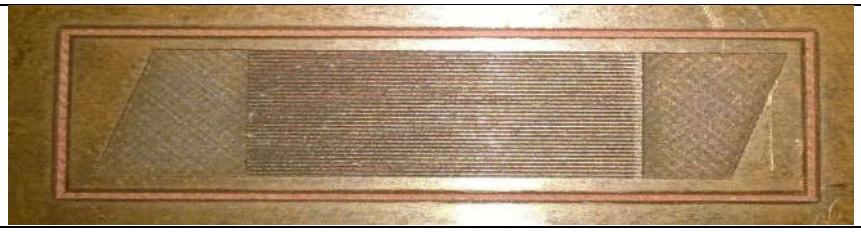

Photo for Case 1: conventional micro channel evaporator.

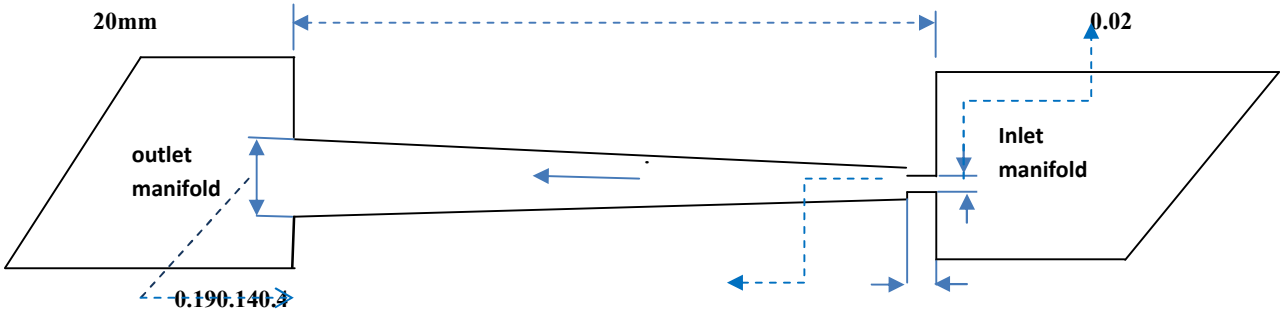

Fig.(3b): geometrical dimensions of Case-2 (one path)

Photo for Case 2: Orifice inlet micro-channel evaporator.

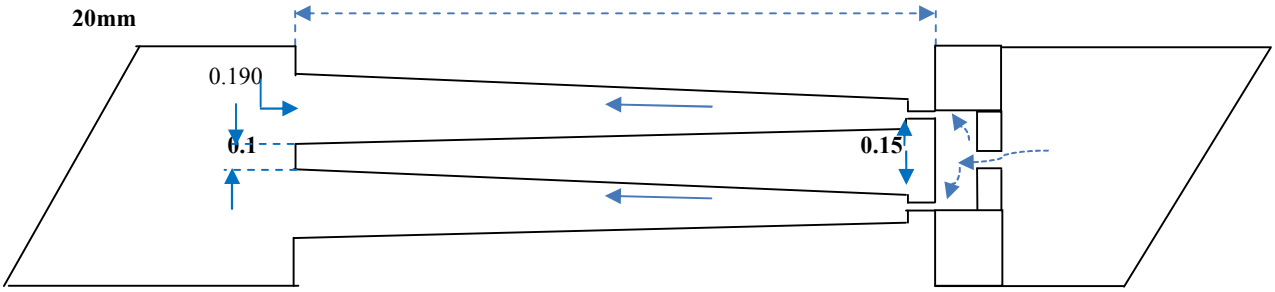

Fig.(3c): geometrical dimensions of Case-2(for one tree only)

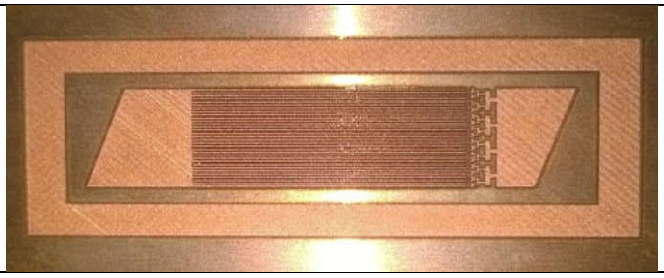

Photo for Case 3: Tree inlet micro-channel evaporator.

The present experimental work is focusing onthe evaporation of a liquid refrigerant inside micro-channel evaporators with different geometries (3 cases).Where,evaporation processwithout the presence of bubbles at the exitwas alsofocused. The present experiments are conducted to compare between the studied three cases in terms of heat transfer coefficient, pressure drop and wall temperature. many test runs are performed at different mass fluxes and heat fluxes.

For the studied three cases, to understand and analyze the results, the boiling flow pattern and its transition is introduced first as shown in figure(5). Then the other results are introduced in the following logic sequence:

1-The variation of heat transfer coefficient (h) versus heat flux (q), vapor quality(x), and wall temperature (T_W) are presented for the studied three cases as shown in Figures (6-a, b,c) for mass fluxes G=400, 900, 1350 $Kg.m^{-2}.S^{-1}$ respectively. Also, the same for pressure drop variation with heat flux (q), vapor quality(x) as presented in Figures (7and 8)at G=400, 900, 1350 $Kg.m^{-2}.S^{-1}$ respectively.

2-As the wall temperature (T_W) is so important parameter in the electronic cooling applications, the variation of both of q with T_W is also included for the studied three cases (figures 9) and at G=400, 900, 1350 $Kg.m^{-2}.S^{-1}$respectively.

3-In addition, the variation of the thermal resistance (R_{th}) with q as plotted in figures (10) at G=400, 900, 1350 $Kg.m^{-2}.S^{-1}$ respectively.

Now, the discussion of figures are given below:

-It is obvious from figure (5) that the flow regime during boiling heat transfer is slug, semi-annular and annular flow, which are characterized by a higher boiling heat transfer coefficient.

-In discussing figures (6) with figure(7), it is clear that the h increases with increasing q for all cases. Also, the ΔP increases as a penalty for all cases. In addition, the highest records of h are obtained at $G=900Kg.m^{-2}.S^{-1}$ as summarized below:

Case	h, $KW.m^{-2}.K^{-1}$	q, $W.cm^{-2}$
Case1(conventional)	h=79	q=165
Case-2(orifice inlet)	92	194
Case-3 (Tree inlet)	109	172

Similarly , the highest records of q are obtained at $G=1350Kg/m^2.S$ as tabulated below:

Case1(conventional)	q=260 $W.cm^{-2}$	h=77$KW.m^{-2}.K^{-1}$
Case-2(orifice inlet)	261	85
Case-3 (Tree inlet)	258	78

As discussed above, Case-3 has achieved the highesthat q=172 $W.cm^{-2}$and $G=900Kg.m^{-2}.S^{-1}$. On the other hand, Case-2 has achieved the highest h ($85KW.m^{-2}.K^{-1}$) at q=261 W/cm^2 and $G=1350Kg.m^{-2}.S^{-1}$.

Conclusion: The Performance of multi micro-channel evaporator has been studied experimentally. Three cases are studied: orifice inlet micro-channels (Case-2), tree inlet micro channels (Case-3) and conventional inlet microchannels (Case-1). It is concluded that:

1-Generally, the problems of refrigerant mal-distribution in microchannel , Reverse vapor flow and boiling fluctuations can be solved by using orifice and tree at inlet to microchannels (Case-2 and Case-3).

2- The highest record of heat transfer coefficient (h=109 KW.m-^{2}.K^{-1}) is obtained at mass flux of (G=900Kg.m^{-2}.S^{-1}) from case-3

Case	h,KW.m^{-2}.K^{-1}	q, W.cm^{-2}
Case1(conventional)	h=79	q=165
Case-2(orifice inlet)	92	194
Case-3 (Tree inlet)	109	172

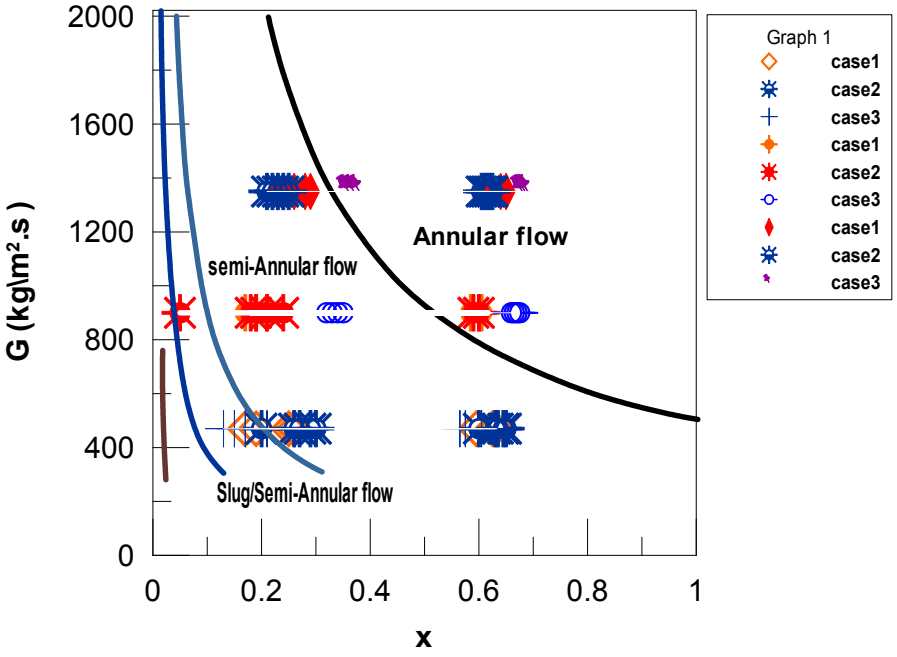

Fig(5) : flow pattern for the studied three cases at different mass fluxes (the solid lines is taken from [3].

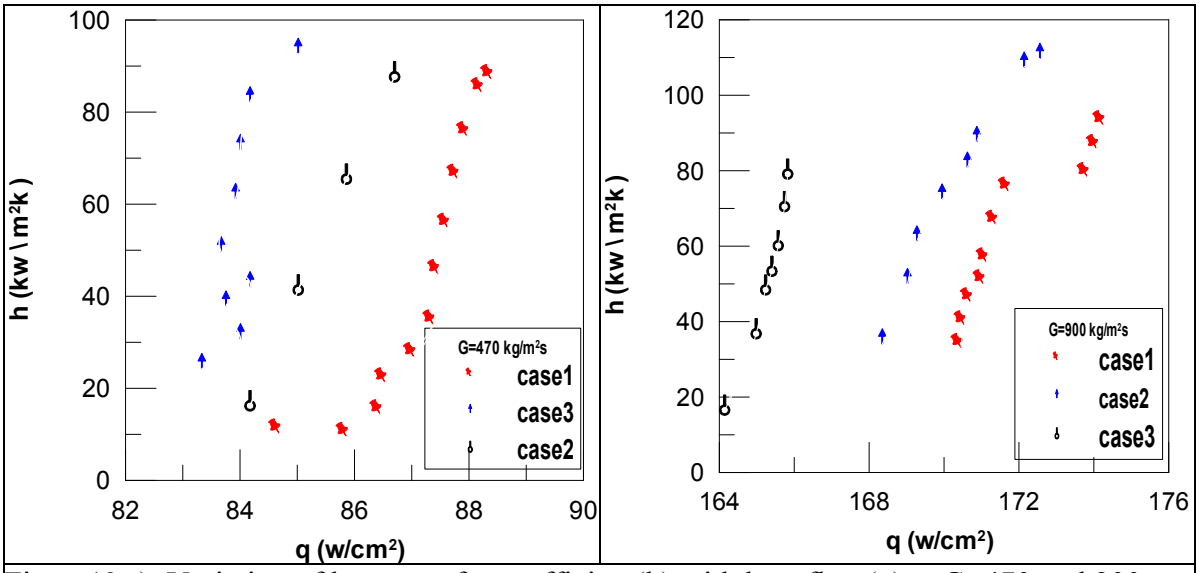

Figure(6-a): Variation of heat transfer coefficient(h) with heat flux (q) at G=470 and 900 Kg.m^{-2}S^{-1} mass fluxes for the studied three cases.

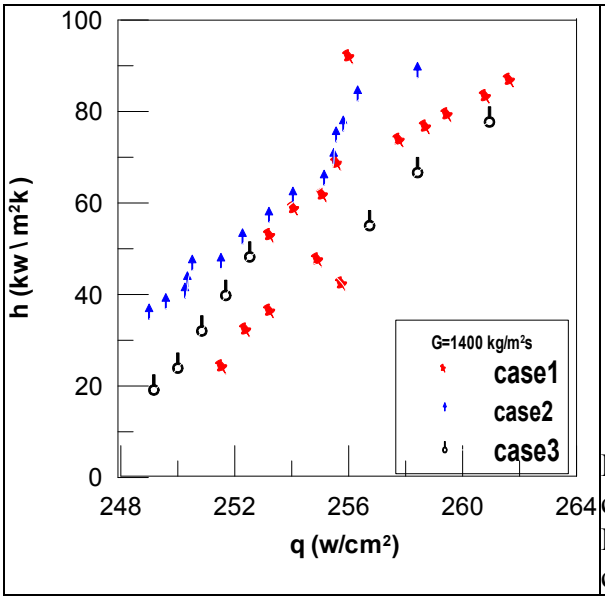

Figure(6-a): Variation of heat transfer coefficient(h) with heat flux (q) at atG=1400 $Kg.m^{-2}S^{-1}$ mass fluxes for the studied three cases

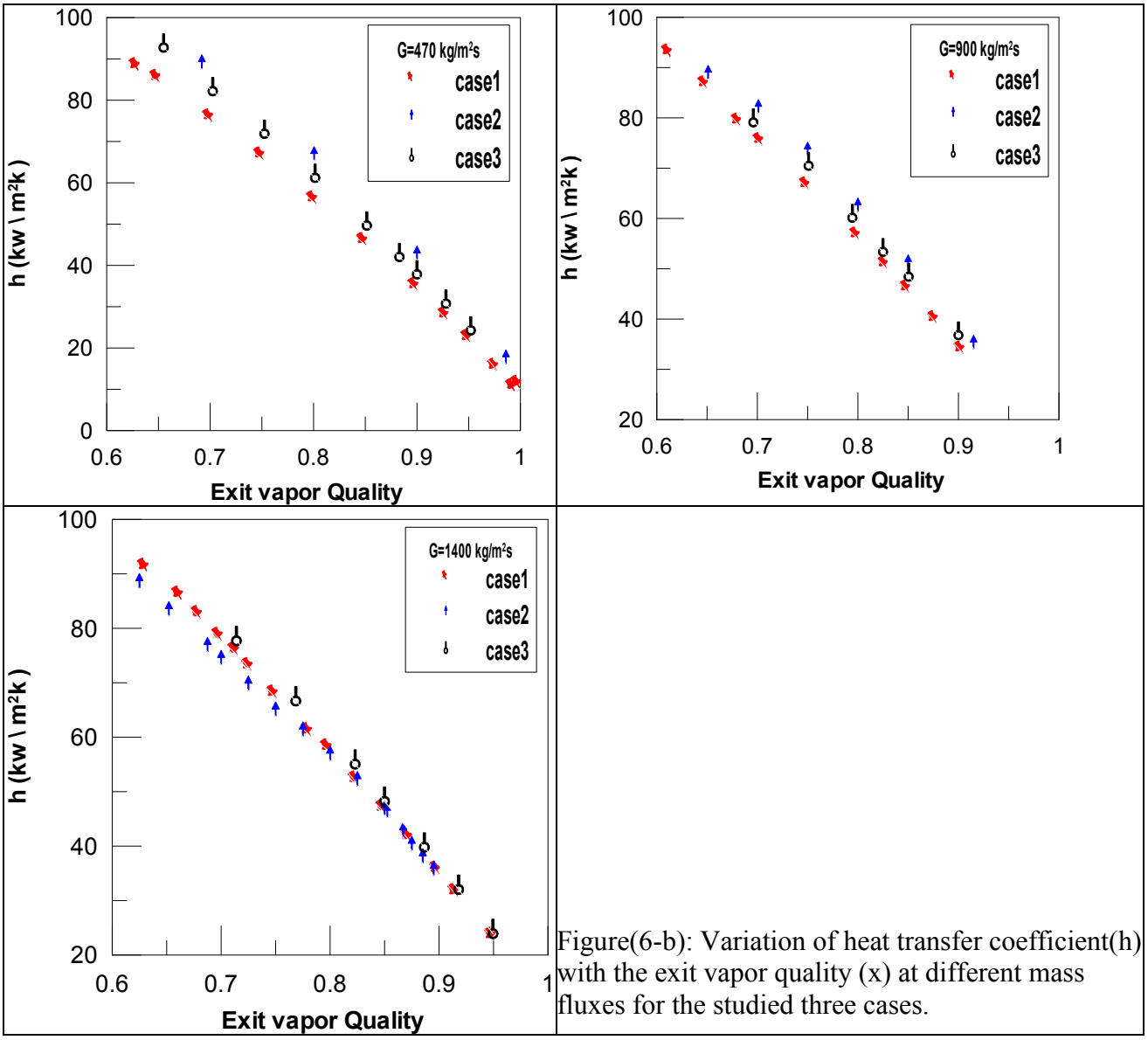

Figure(6-b): Variation of heat transfer coefficient(h) with the exit vapor quality (x) at different mass fluxes for the studied three cases.

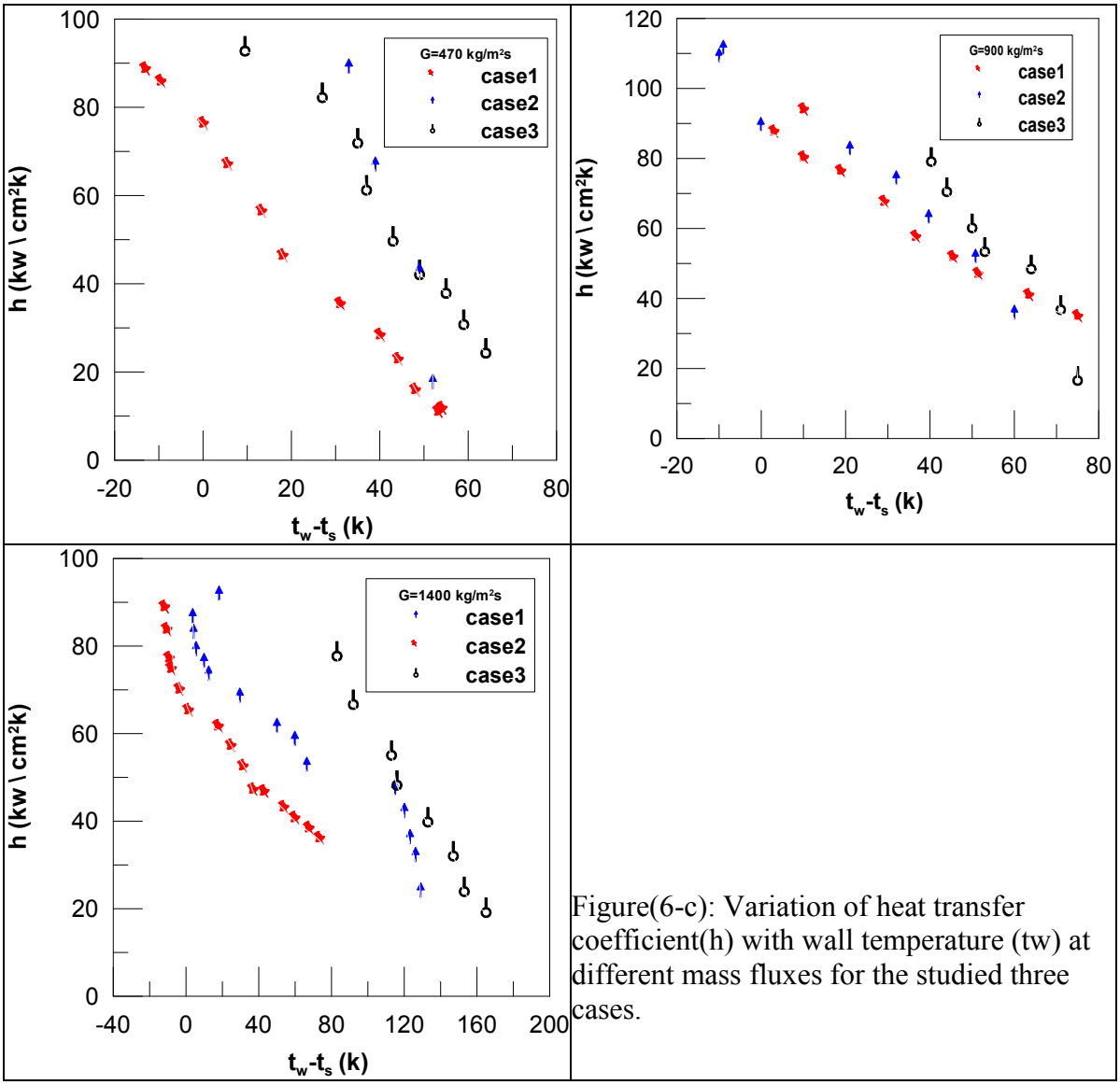

Figure(6-c): Variation of heat transfer coefficient(h) with wall temperature (tw) at different mass fluxes for the studied three cases.

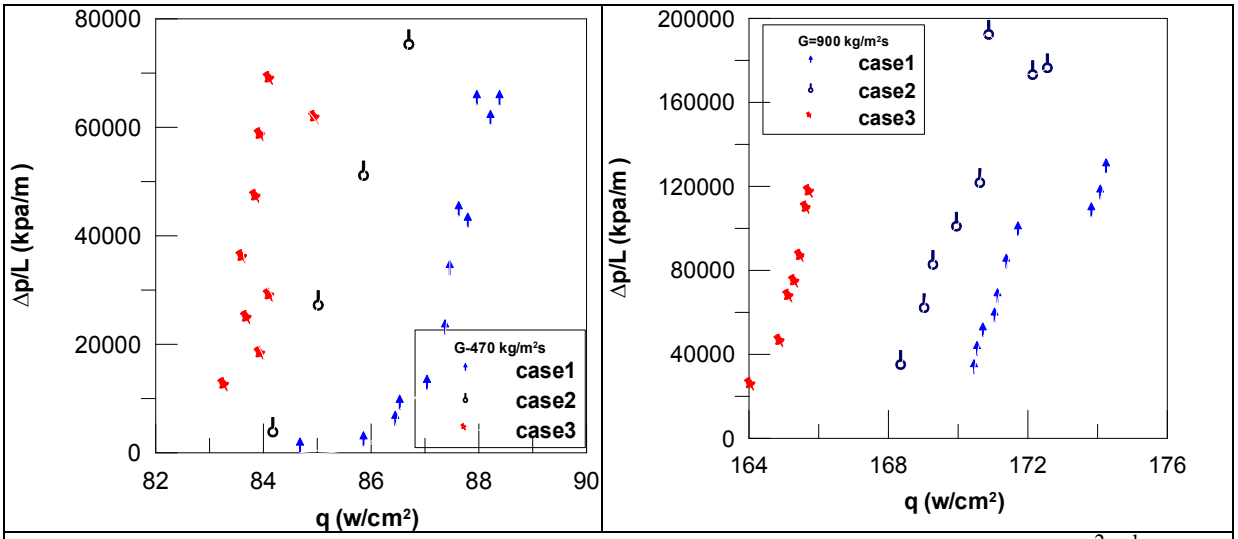

Figure(7): Variation of pressure drop(ΔP) with heat flux (q) at G=470 and 900 Kg.m^{-2}S^{-1} for the studied three cases.

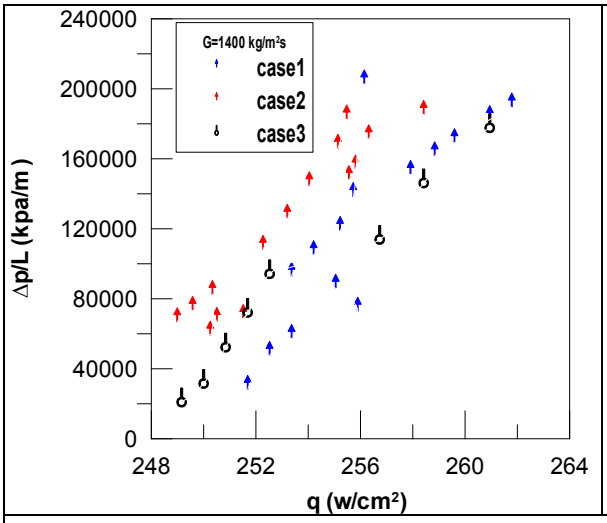

Figure(7): Variation of pressure drop(ΔP) with heat flux (q) at G=1400 $Kg.m^{-2}S^{-1}$ for the studied three cases.

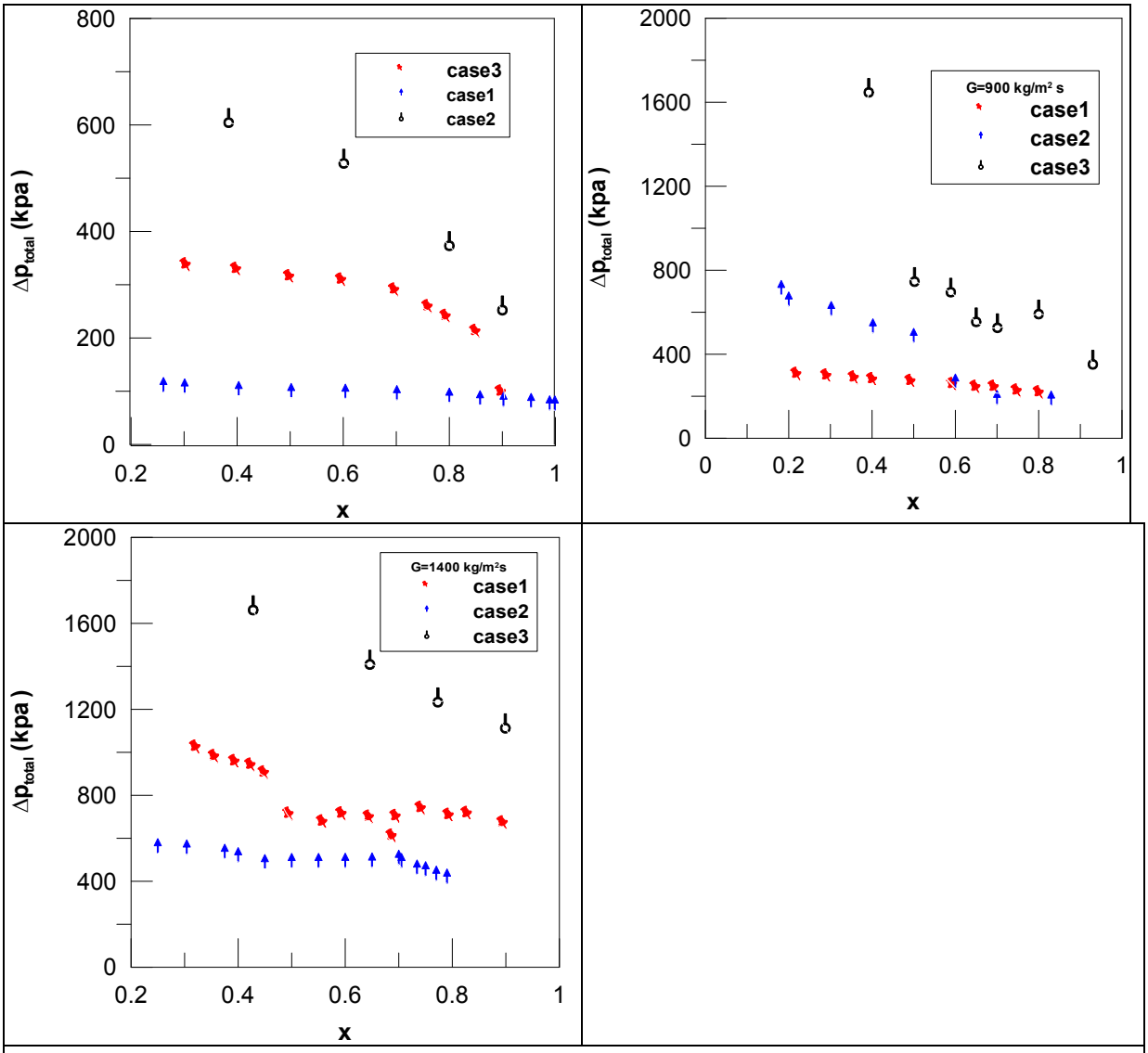

Figure(8): Variation of pressure drop(ΔP) with vapor quality (x) at different mass fluxes for the studied three cases.

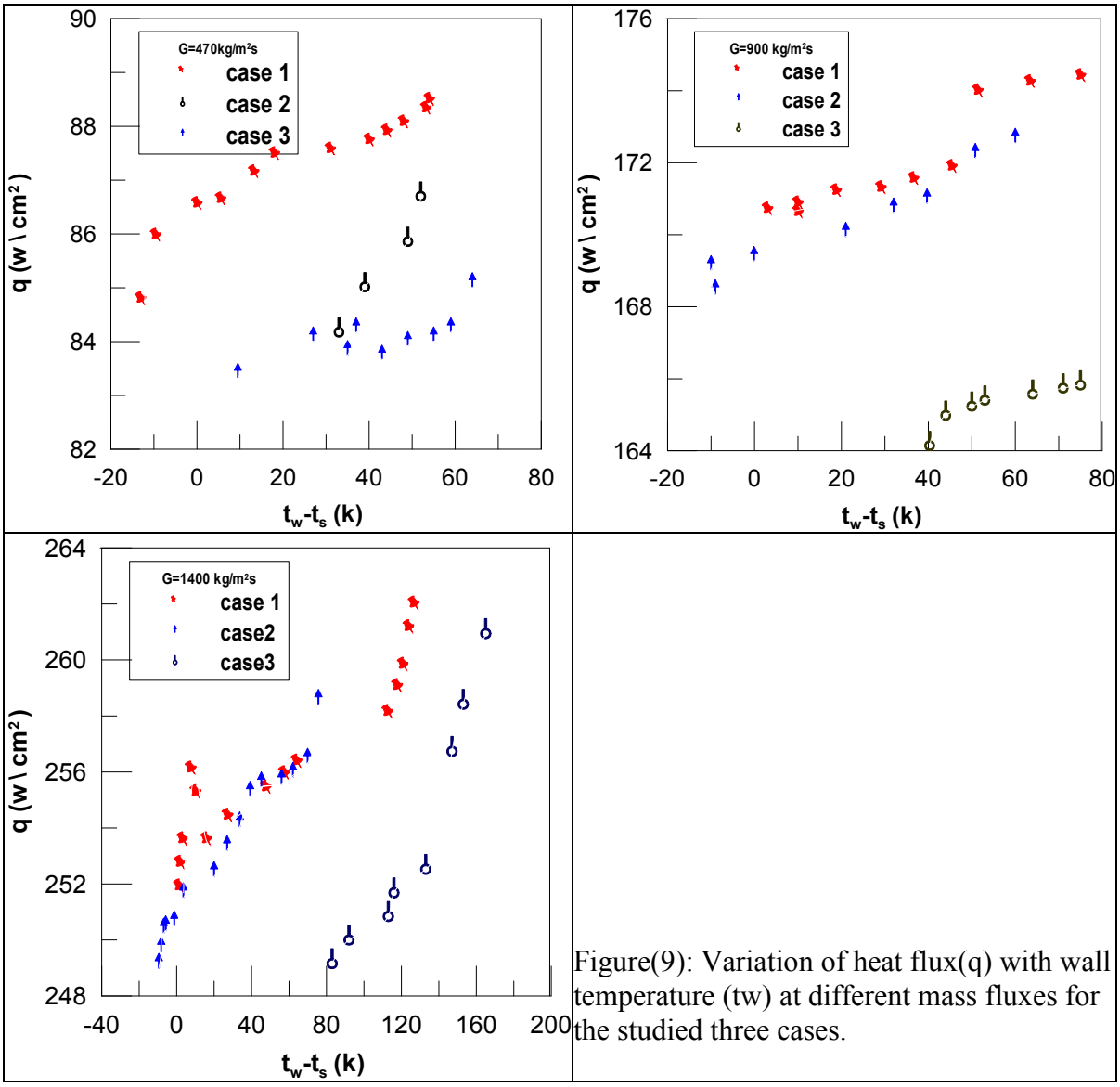

Figure(9): Variation of heat flux(q) with wall temperature (tw) at different mass fluxes for the studied three cases.

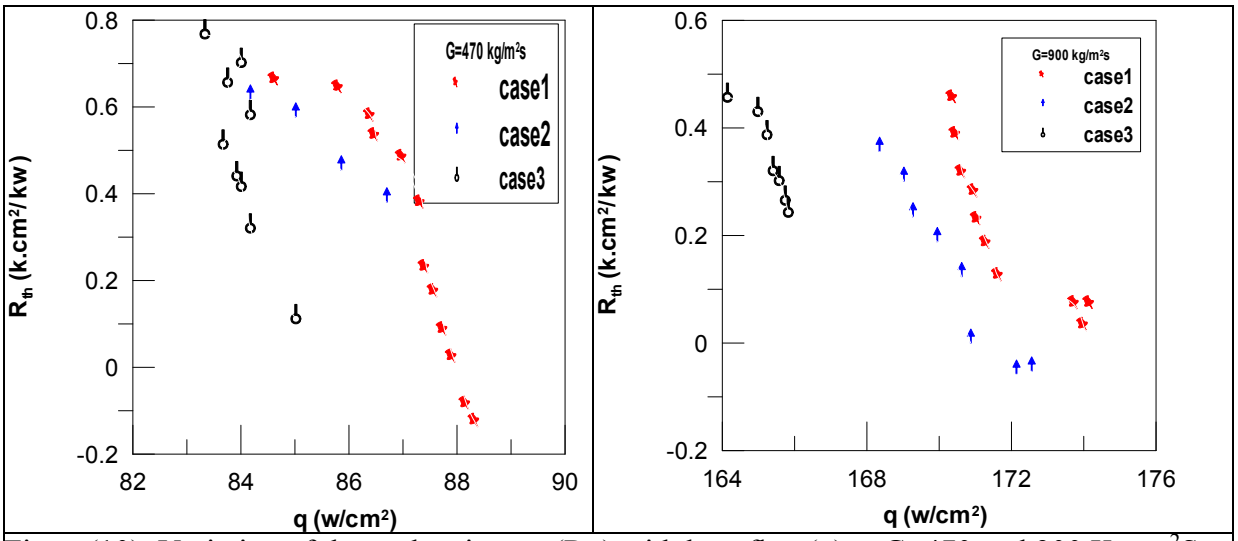

Figure(10): Variation of thermal resistance(R_{th}) with heat flux (q) at G=470 and 900 $Kg.m^{-2}S^{-1}$ for the studied three cases.

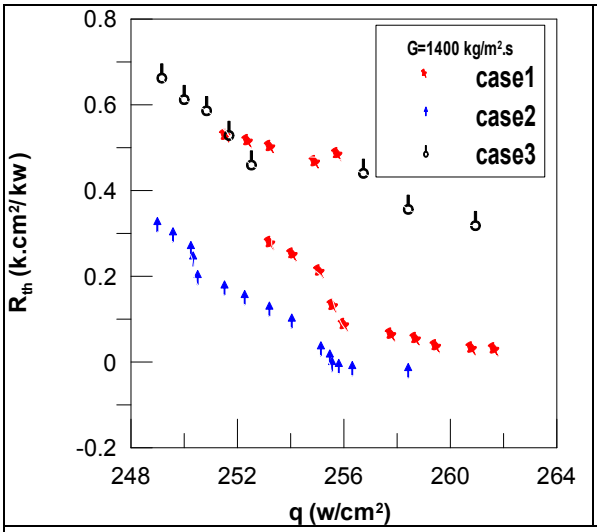

Figure(10): Variation of thermal resistance(R_{th}) with heat flux (q) at G=1400 $Kg.m^{-2}S^{-1}$ for the studied three cases.

References

[1] Tannaz H. and Suresh V., 2011 "Boiling Heat Transfer and Flow Regimes in Microchannels : A Comprehensive Understanding" Journal of Electronic Packaging, Vol. 133.

[2] Yifan L., Guodong X., Yuting J., 2017"Experimental investigation of flow boiling performance in microchannels with and without triangular cavities : A comparative study"International Journal of Heat and Mass Transfer 108 , P: 1511–1526.

[3] Kandlikar, S., Grande, W., 2002 " Evolution of microchannel flow passages thermo hydraulic performance and fabrication technology " ASME International Mechanical Engineering Congress & Exposition November 17-22.

[4] Balasub, P. and Kandlikar S., 2005 " Experimental study of flow patterns, pressure drop, and flow instabilities in parallel rectangular minichannels" Heat Transfer Eng., 26(3): 20-27.

[5] Bergles, A, and Kandlikar S., 2005 " On the nature of critical heat flux in microchannels" journal of Heat Transfer, 127(1): 101- 107.

[6] Kandlikar, S., Kuan W., Willistein D., and Borrelli H., 2006 "Stabilization of flow boiling in microchannels using pressure drop elements and fabricated nucleation sites" Heat Transfer, 128(4) : 389–396.

[7] Kalani A., Kandlikar S., 2015 "Effect of taper on pressure recovery during flow boiling in open microchannels with manifold using homogeneous flow model" Heat Mass Transf. 83 : 109–117.

[8] Kandlikar S. , 2004" Heat transfer mechanisms during flow boiling in microchannels" Heat Transfer, V. 126, pp. 8-16

[9] Sempértegui D., and Ribatski D., 2017 " Flow boiling heat transfer of R134a and low GWP refrigerants in a horizontal microscale channel" Heat Transf. 108 : 2417–2432.

[10] Ahmet S., Cansu Ö., 2018 " Experimental investigation on the flow boiling of R134a in a multimicrochannel heat sink" Heat Transfer: 125–137

[11] Xuejiao L., 2018"Effect of flow instability on flow boiling friction pressure drop in parallel micro-channels" Heat Mass Transfer : 64–71.

[12] Hrnjak H., 2017 " Visualization and measurement of reverse flow in an actual channel of a microchannel evaporator" Heat Mass Transf. 108.

[13] Hrnjak H., 2018 "Heat transfer and pressure drop of R32 evaporating in one pass microchannel tube with parallel channels" Heat Mass Transfer, 127.

[14] Hrnjak H., 2019 "Flow visualization of R32 in parallel-port microchannel tube" Heat Mass Transfer: 128 : 1–11.

[15] W. L, Wu , 2010 "A general correlation for evaporative heat transfer in micro/minichannels" Heat and Mass Transfer, 53: 1778– 1787.

[16] Tibiriçá C., Ribatski G., 2014" Flow patterns and bubble departure fundamental characteristics during flow boiling in microscalechannels:Exp" Therm. Fluid , 59 : 152–165.

[17] Zhang P., Jia H., 2016 " Evolution of flow patterns and the associated heat and mass transfer characteristics during flow boiling in mini-/micro-channels" Chem. Eng, 306 : 978–991.

[18] Magnini M., Thome H., 2013 "Numerical investigation of the influence of leading and sequential bubbles on slug flow boiling within a microchannel" Therm. Science, 71 : 36–52.

[19] Rahim, E. , Bar-Cohen A., 2015 "Thermal characteristics of a chip-scale two-phase microgap cooler" Heat Transfer Engineering , 36: 511–520.

[20] Green C., Kottke E., Bakir M. , 2015 "A review of two-phase forced cooling in three-dimensional stacked electronics: technology integration" Electron. Packag. , 137 , 4: 040802.

[21] Hrnjak H., 2017 "Visualization and measurement of reverse flow in an actual channel of a microchannel evaporator" Heat Mass Transf. 108 : 2346–2354.

[22]Ali, R. (2010) "Phase change phenomena during fluid flow in micro channels " Doctoral Thesis, Department of Energy Technology, Royal Institute of Technology, Stockholm, Sweden.